ELSEVIER

PII:S0144-8617(96)00014-8

Carbohydrate Polymers 29 (1996) 137–148

0144-8617/96 $15.00+.00

Small deformation rheological properties of maltodextrin–milk protein systems

Ioannis S. Chronakis, Stefan Kasapis* & Robert K. Richardson

Department of Food Research and Technology, Cranfield University, Silsoe College, Silsoe, Bedford, MK45 4DT, UK

(Received 14 June 1995; revised version accepted 13 September 1995; accepted 15 September 1995)

Small deformation dynamic oscillation was used to investigate the structural behaviour of conformationally dissimilar maltodextrin and milk protein macromolecules in a mixture, with the view of identifying the state of phase separation and the pattern of solvent distribution between the two constituent phases. The enthalpic nature of the maltodextrin network produced a sigmoidal transition in the development of storage modulus (G') during cooling and substantial thermal hysteresis upon heating of the gel. By contrast, the entropically-driven build up of structure in milk protein samples yielded linear and overlapping cooling and heating scans of G' with networks reverting into solutions at relatively low temperatures. These differences in the viscoelastic functions of the two polymers in combination with theoretical analysis (isostress–isostrain models, Kerner equation) have documented the reinforcing effect of strong and spherical maltodextrin inclusions on the weaker and continuous milk protein phase. However, at concentrations of maltodextrin beyond the phase inversion point, the binary assembly comprises a strong and continuous maltodextrin network surrounding the weaker milk protein inclusions. Finally, the sharp change in the pattern of water partition between the two polymeric components, as a result of phase inversion in the system, was rationalised on the basis of kinetically-influenced co-gels comprising phase separated networks which are trapped away from the state of thermodynamic equilibrium. Copyright © 1996 Published by Elsevier Science Ltd

INTRODUCTION

The commercial development of the functional food concept saw the use of polysaccharide–protein and protein–protein mixtures as structuring ingredients of reduced calorie products. Blends of maltodextrin–gelatin, maltodextrin–milk protein and milk–soya protein systems are the favourite fat replacers especially in the production of low fat spreads and soft cheeses (Daniels *et al.*, 1993; Banach *et al.*, 1993).

The structural properties of single and mixed gels of limed ossein gelatin and Paselli maltodextrin with a dextrose equivalent DE (which gives the number of reducing end groups relative to glucose as 100), of 2.9 (SA-2) and 4.3 (SA-6) were recently investigated (Kasapis *et al.*, 1993a). Depolymerisation of potato starch to maltodextrin results in relatively small molecular weight molecules, e.g a hydrolysate of DE 2.9 is a species with a number average of 35 residues per chain which requires relatively high concentrations for gelation (about 10%). Gelatins, of course, form soft gels at a tenth of this amount (about 1% polymer). Controlled heating reveals that maltodextrin aggregates are much more heat resistant than the gelatin triple helix, with networks reverting to solutions at 80 and 30°C, respectively (scan rate of 1 deg/min). Mixed solutions show signs of bulk phase separation upon centrifugation at temperatures where the individual components remain stable as disordered coils (Kasapis *et al.*, 1993b). Thus, concentrated preparations resolve into two liquid layers at equilibrium whose composition defines a cloud point curve, or produce an insoluble maltodextrin precipitate. Combined evidence of gel-time measurements, light microscopy, differential scanning calorimetry, and the temperature-course of gel melting demonstrated that composite gels phase invert over a narrow concentration range from gelatin continuous mixtures to systems at which maltodextrin constitutes the supporting matrix (Kasapis *et al.*, 1993c). Experimental observations below the phase inversion point were rationalised quantitatively on the basis of a continuous gelatin network, which undertook gradual deswelling due to ordering of the slower gelling maltodextrin component (Kasapis *et al.*, 1993d). This idea is compatible with the starting position of a clear, single-phased solution of coexisting, disordered maltodextrin and gelatin chains observed at high temperatures. At

*To whom correspondence should be addressed

combinations beyond the phase inversion point, however, results were better described by the assumption of immediate phase separation of the cloudy solution into a continuous, maltodextrin-rich phase surrounding the gelatin-rich droplets at thermodynamic equilibrium. Subsequent cooling produced a mixed gel with a supporting maltodextrin matrix, but the different gelation rates between the two polymers have posed the question of kinetic effects on the resulting composite structure. Analysis of milk and soya protein systems also demonstrated that the conformationally similar globular proteins tolerate each other in a single phase at low solid levels whereas at higher concentrations the polymers resolve into two discrete liquid layers at equilibrium (Chronakis & Kasapis, 1993). Again, to what extent this state of equilibrium had been disturbed by gelation during cooling of the phase-separated protein solution remained largely unresolved.

The present work examines the case of non-equilibrium influences on the partition of water between the maltodextrin and milk protein networks. It also investigates how differences between the network of associated amylose-like double helices and the corpuscular aggregates of thermally unfolded protein molecules effect changes in the phase state of their blends. In both cases, characterisation of the physical properties of single maltodextrin and milk protein gels is needed as a reference for the study of mixed systems. Obviously, a good understanding of the above and of the technical approaches involved will also assist the food scientist in placing the development of novel products on a sound technological basis.

MATERIALS AND METHODS

The maltodextrin used in this investigation is marketed as a white, odourless powder by Cerestar Ltd, Trafford Park, Manchester, UK, under the name C* Pur 01906, batch number YH1155. It is a neutral dextrin prepared from potato starch by a special process involving a continuous enzyme hydrolysis (α-amylase from *Bacillus subtilis*) at the gelatinisation temperature (about 75°C). Following this, the enzyme is inactivated at pH 3.5 and the sample is neutralised for subsequent spray drying under vacuum at 80°C. Gel permeation chromatography (GPC) has indicated a dextrose equivalent number of 3.9, meaning that there are on average 26 glucose molecules per chain. Slicing of the GPC spectrum produced the following molecular weight distribution:

M_w	Area (%)
$< 10^3$	5.19
$1–5\times10^3$	18.27
$5–25\times10^3$	26.38
$25\times10^3–2\times10^5$	44.54
$2\times10^5–10^6$	5.56
$10^6–5\times10^6$	0.06

The commercial milk concentrate used was supplied by Ingredia Ltd, Early, Reading, UK and it is traded under the name Promilk 602. Physico-chemical analysis produced the following specification: 60% protein, 25.5% lactose, 8% ash and 1.5% fat. The moisture content of the sample is 5%. Its production initially involves ultrafiltration of skim milk using a membrane filter with a molecular weight cut-off of 10,000. Subsequent spray drying at about 80°C causes whey protein denaturation as well as promoting covalent interactions between whey protein and casein molecules.

Protein samples were easily prepared by dispersing the powder in distilled water at 50°C whereas dissolution of maltodextrin required rigorous mechanical stirring at 90°C. Binary systems were produced by mixing appropriate amounts of stock preparations at 50°C. Measurements of dynamic oscillation were made on a controlled stress Carri-Med CSL500 rheometer, using parallel plate geometry of 40 mm diameter and 1 mm gap. Single and mixed preparations were loaded on the pre-heated platen at 50°C and were cooled to 5°C at a scan rate of 1 deg/min and frequency of 1.6 Hz.

The applied deformation was fixed at 1% strain which was well within the linear viscoelastic region for both gels of milk protein (Chronakis & Kasapis, 1993) and maltodextrin. In Fig. 1, increasing amounts of the carbohydrate create more aggregated (i.e. more heterogeneous) networks which exhibit higher strain sensitivity shown by a diminishing linear viscoelastic response (from about 10 to 2% strain at 20 and 50% maltodextrin, respectively). For the 50% sample, recording stopped at 2.48% strain due to exhaustion of the available stress on the rheometer.

Temperature was controlled by a Pt100 thermometer

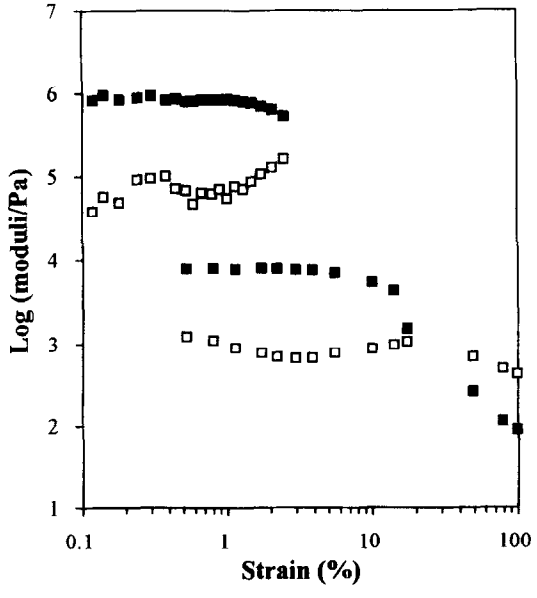

Fig. 1. Strain sweeps of G' (■) and G'' (□) for 20 and 50% maltodextrin gels (bottom and top spectrum, respectively), at a frequency of 1.6 Hz.

in a Peltier device and the loss of water or absorption of atmospheric moisture was minimised by applying a layer of silicone fluid (50 cs) to the exposed edges of the sample. Cooling scans were followed by a 90 min isothermal run at 5°C. Lastly, samples were heated to 95°C at the same rate of 1 deg/min. The above sequence of experimental procedures allowed recording of the development and demise of the storage modulus (G'), loss modulus (G'') and complex dynamic viscosity (η^*) as functions of time and temperature.

RESULTS AND DISCUSSION

Low amplitude oscillatory properties of maltodextrin gels

Previous studies of maltodextrin gelation on Paselli SA-2 and SA-6 have shown substantial differences in the pattern of network development for the two homologues (Kasapis *et al.*, 1993a). Thus the shorter segments of SA-6 produce a linear concentration (C) to modulus dependence which indicates dominant frictional forces between adjacent particles of aggregated helices. However, the longer chains of SA-2 seem capable of forming a network according to the approach proposed by Clark & Ross-Murphy (1985). Briefly, the network connectivity in this model is defined by the valency of binding sites per macromolecule (functionality, f), the degree of cross-linking of functionalities (conversion factor, α), the proportion of elastically ineffective network chains (extinction probability v), and the equilibrium constant (K) between ordered and disordered chain segments. Based on these parameters the G' vs C function is given by the following mathematical expression:

$$KG'(f-1)(f-2)/gRT = \{C/C_O\} \{[(f-1)^2\alpha(1-v)^2(1-\beta)]/[2(f-2)]\} \quad (1)$$

where g is the "front factor" which scales the absolute value of modulus, R is the gas constant, T is the absolute temperature of the gel and the β parameter is a function of α, f and v. On a log G' vs C plot, the fit transforms from a linear dependence at higher concentrations to a sharp curvature which continues until the minimum critical concentration of the polymer is reached (C_O; the slope of modulus growth tends to infinity in Ross-Murphy, 1991).

The above body of theory has been used to relate the modulus with concentration for the maltodextrin sample of the present investigation. In doing so, the combined temperature and time course of gelation was monitored for polymer levels in the range from 14 to 50% (typical traces are shown in Fig. 2). The onset of gelation is heavily governed by concentration with the 15% preparation producing an extended "lag period" of $\approx$ 67 min whereas at 50% solids G'

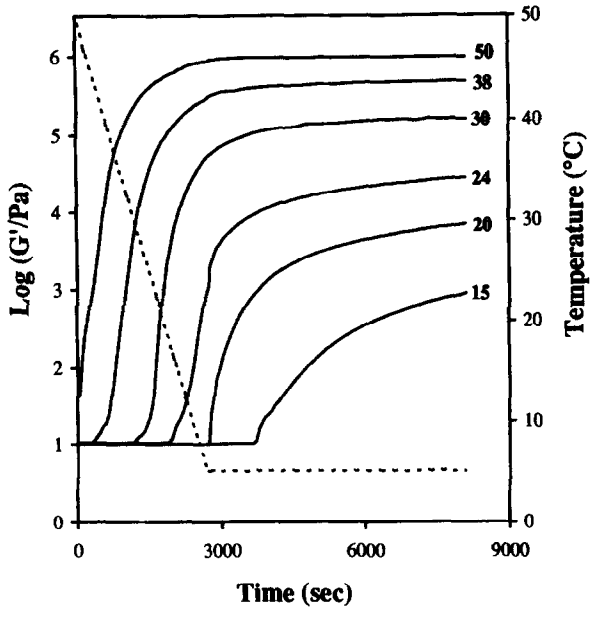

Fig. 2. Combined controlled cooling of maltodextrin samples (% w/w) from 50 to 5°C at 1 deg/min and isothermal run at 5°C for 90 min (frequency of 1.6 Hz; 1% strain).

increases as soon as the cooling down commences. On the whole, gel formation shows a sigmoidal building of mechanical strength which is characteristic of evolving enthalpic associations in carbohydrate networks (Ptitchkina *et al.*, 1994). The internal rearrangements and structure of the gels seem to settle within the experimental timescale for the great majority of samples, as indicated by the moduli traces which asymptotically approach constant values, although there is some gradient in the isothermal development of G' for the 15% preparation. Frequency sweeps at the end of the run at 5°C produced flat spectra characteristic of gels with a high solid character. Figure 3 illustrates typical responses with the ratio of G'' to G' (tan δ) at 1.6 Hz obtaining values of 0.03 and 0.09 for the 50 and 24% maltodextrin networks, respectively.

Figure 4 shows the heating profiles of storage modulus for maltodextrin gels which have been treated with the experimental conditions specified in Fig. 2. Surprisingly, the melting curves show a unique feature in addition to the expected increase in melting temperature (t_m) with maltodextrin concentration (t_m values have been found to vary from 70 to about 95°C for other potato maltodextrins; Kasapis *et al.*, 1993c). Thus, the temperature course of gel melting changes with increasing concentration from a smooth, progressive reduction in G' (up to about 20% polymer) to a two-step decrease in network strength, with by far the biggest part of structure collapsing within the first stage.

Fitting the concentration dependence of shear modulus (values taken at the end of the isothermal run in Fig.

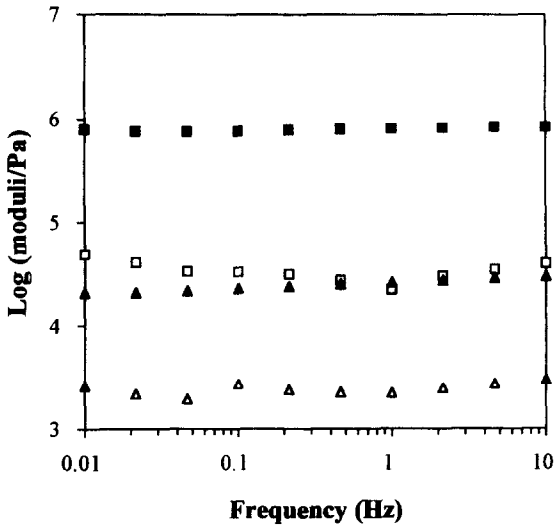

Fig. 3. Mechanical spectra obtained for 24% maltodextrin [G'(▲); G''(△), and 50% maltodextrin [G'(■); G'' (□)] gels, at a strain of 1% (5°C).

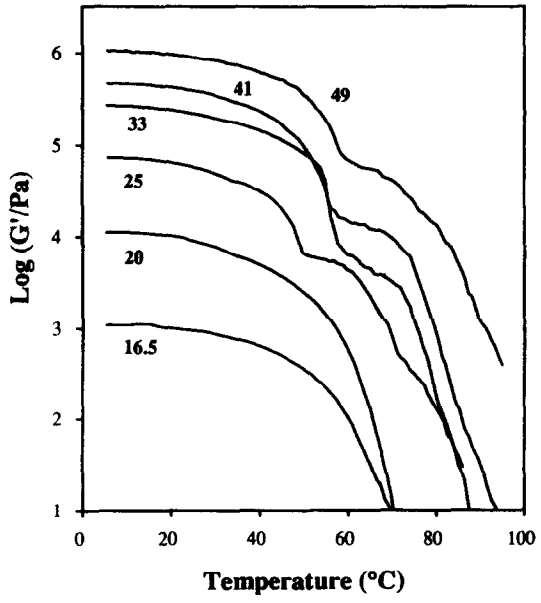

Fig. 4. Controlled heating of maltodextrin gels (% w/w) from 5 to 95°C at a scan rate of 1 deg/min, following the experimental procedures of Fig. 2 (frequency of 1.6 Hz; 1% strain).

2) with the mathematical expression of the cascade theory (eqn 1) provided evidence of the phenomenon behind the unusual thermal failure of C^*1906 gels. Attempts to establish a unique relationship between G' and C throughout the concentration range yielded calculated values that failed to trace the pattern of experimental data, as indicated by the unacceptably high sum (1.22) of minimised differences of $[\log G'_{calc} - \log G'_{exp}]^2$ in a least squares fit (Fig. 5). Pondering over the transformation from a single to a bimodal melting behaviour in Fig. 4 we decided to fit separately the concentration ranges of 14–20% and 21–50%. As shown in Fig. 5, the result was two very good fits with the sum of squared differences being equal to 0.04 and 0.09 for the bottom and top concentration ranges, respectively. Therefore, the unusual heating feature of this maltodextrin is reflected on a $G'(C)$ function that shows a discontinuity at the vicinity of a concentration (about 20%) associated with the emergence of a two-step melting curve.

Recently, Kasapis *et al.* (1993b) have argued that the mechanism of network formation for maltodextrins can

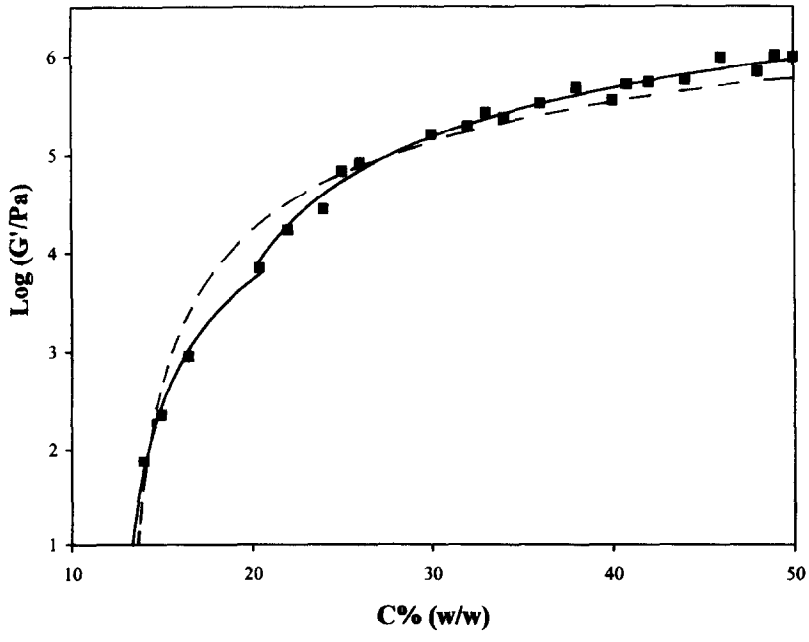

Fig. 5. The blending of two cascade treatments in a concentration-storage modulus continuum for the maltodextrin gels of Fig. 2 at the end of the time scan (5°C; 90 min). The dashed line shows an earlier attempt to fit the full set of points with a single cascade treatment.

be inferred from the gelation of starch which is based on creation of co-axial double helices by 1,4-linked α-D-glucan chains and the lateral aggregation of these intermolecular associations (Gidley, 1989). The chromatogram of the present maltodextrin sample shows that there is a core of high molecular weight chains (about 6% between 2×10^5 and 5×10^6) capable of forming ordered nuclei for the development of a three-dimensional network. Shorter chains are not likely to participate in the initialisation of multifunctional junction zones, with an average helix length of about 70 residues being required for commencing of the nucleation process (Jane & Robyt, 1984; Clark *et al.*, 1989). However, it was found that linear oligomers with a M_w down to 1000 can crystallise with segments of preformed helices thus contributing to the mechanical strength of the network (Gidley & Bulpin, 1987). The effect of addition of short species should be significant for this batch of maltodextrin since it contains about 32% more material than the typical C^*1906 preparation within the M_w range from 1000 to 5000, i.e. for molecules of seven to thirty five glucose units (F. Deleyn, personal communication). The length and therefore the stability of these associations is limited by the length of the shorter partner which convert to the disordered state at lower temperatures than their longer counterparts, hence producing the two-tiered melting profile of Fig. 4. Similarly, the two-step development of shear modulus as a function of concentration in Fig. 5 should be due to the transition from high molecular weight assemblies to large aggregates comprising long helices, and short linear and branched chains. Along these lines, the first wave of structural loss during a heating run abolishes the bulk of peripheral associations leaving intact the intermolecular associations of long strands. Therefore, networks at the beginning of the second melting process in Fig. 4 should comprise sparsely cross-linked structures of high molecular weight chain segments in the manner envisaged for maltodextrin concentrations of 20% and below.

To double check this proposal, the concentration dependence of elastic moduli derived from networks of presumed long linear chains was plotted in Fig. 6 and fitted using the algorithm of the cascade model (eqn 1). Gratifyingly, a high quality fit was obtained with a low sum of squared moduli differences (0.08), a C_O value of 11.6% and a functionality of about 7. By comparison the minimum critical gelling concentration and the functionality values produced upon fitting the G' values of maltodextrin gels between 21 and 50% in Fig. 5 were 16.2% and $\approx$ 3, respectively. Therefore, the experimental and calculated evidence is entirely consistent with the proposal of thermally-stable long helices acting as the structural units of the C^*1906 network, which however encourages at high levels of solids the close packing of shorter, thermally-metastable segments around the central core of helices.

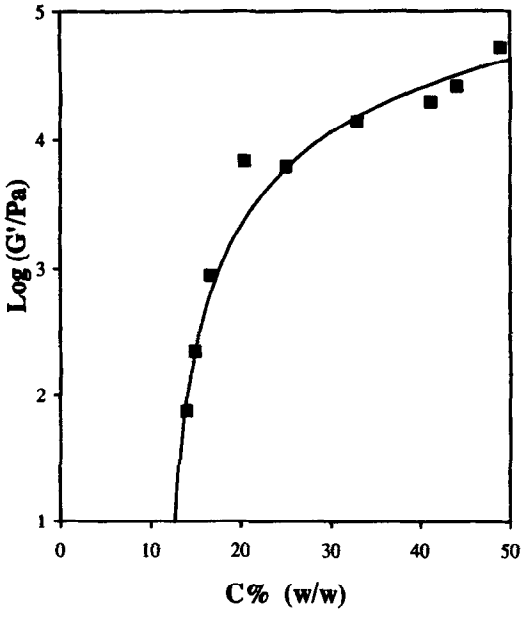

Fig. 6. The cascade modelling of storage modulus derived from maltodextrin gels with a single-stepped heating profile and networks at the beginning of the second step in the melting process.

Characterisation of milk protein gels

The structural properties of milk protein concentrates are governed by the production methods employed, amongst which isoelectric precipitation, ultrafiltration and spray drying are the commonest. Differential scanning calorimetry (DSC) measurements of Promilk 602 have produced featureless thermograms upon heating from 5 to 95°C (Chronakis & Kasapis, 1993). This contrasts strongly with the DSC heating profile of maltodextrin gels in which a broad endothermic event commences at 40°C, shows a midpoint transition temperature at 70°C and concludes at about 95°C, thus revealing order-to-disorder processes in the maltodextrin aggregates (Manoj *et al.*, in press). Obviously, the milk protein of this investigation has been denatured during commercial preparation and remains irreversibly unfolded as observed for the thermal denaturation of other globular proteins (Hermanson, 1978).

For the investigation of small deformation properties of Promilk samples, the temperature and time course of storage modulus was monitored and it is reproduced in Fig. 7. Clearly, there is a linear increase in G' as a function of temperature from 50°C downwards, with a sharp discontinuity at 5°C and no significant further change in network strength during the ensuing isothermal run for 90 min. This pattern of structural development suggests an entropically-driven network which utilizes the reduction in thermal motion upon cooling to form aggregates of closely packed globular macromolecules. The end of the cooling run sees a system with a constant thermal energy content, i.e. a certain attraction–repulsion equilibrium between particles at the reference

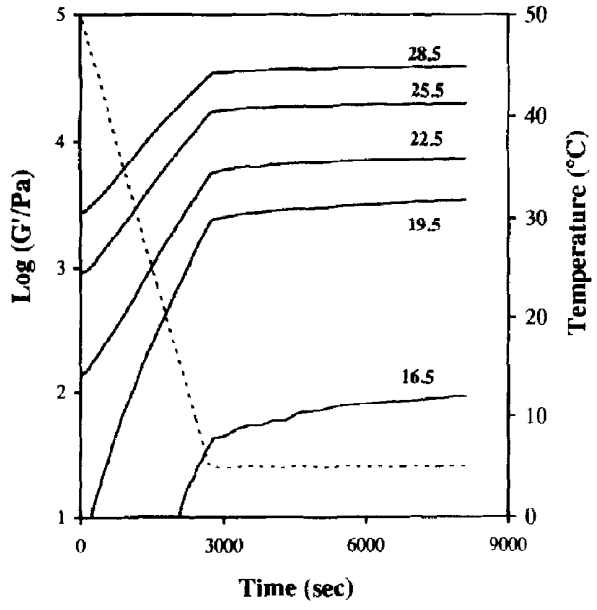

Fig. 7. Combined controlled cooling of milk protein samples (% w/w) from 50 to 5°C at 1 deg/min and isothermal run at 5°C for 90 min (conditions as in Fig. 2).

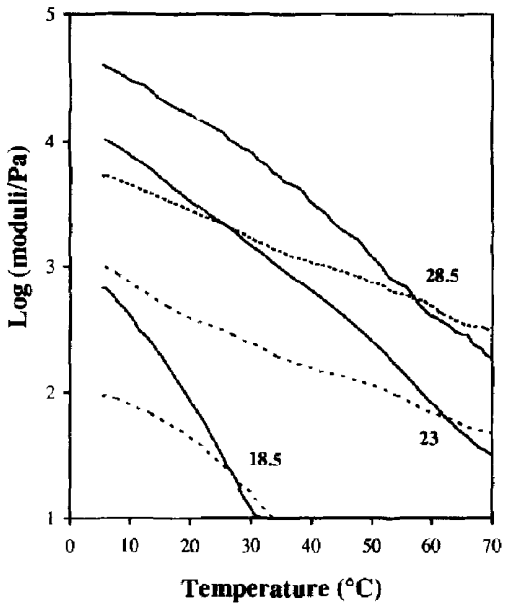

Fig. 8. Heating profiles of G' (–) and G'' (- -) for milk protein gels (% w/w) from 5 to 95°C at a scan rate of 1 deg/min, following the experimental procedures of Fig. 7 (conditions as in Fig. 2).

temperature of 5°C, whose time–temperature manifestation diverges from the sigmoidal, enthalpically-driven gelation process of the maltodextrin polysaccharide in Fig. 2. Mechanical spectra at the end of an isothermal run show a gel-like structure over a four decade frequency range (ω from 0.001 to 10 Hz in Chronakis & Kasapis, 1993). Thus the elastic response dominates over viscous flow with little frequency dependence in either modulus, and the decrease in log η^* is a linear function of log ω. However, the ratio of loss to storage modulus (tan δ is $\approx$ 0.12) reveals that the protein network contains a higher "sol fraction" than those of maltodextrin and other biopolymer gels (tan δ varies from 0.01 to 0.04; Clark *et al.*, 1982).

Figure 8 illustrates the melting profiles taken upon heating the Promilk structures at 1 deg/min, following the frequency sweeps described in the preceding paragraph. Samples lose their structural integrity following the same temperature-course as observed during cooling, hence showing no signs of thermal hysteresis between the developing and diminishing storage modulus. Again this behaviour contrasts strongly with the huge temperature lag observed in Figs 2 and 4 for the setting and melting of maltodextrin samples, being about 65°C for the 20% maltodextrin gel and presumably even higher for the thermally-irreversible structures (e.g. 49% maltodextrin). The linear decline in network strength with temperature means that the system responds readily to the increase in entropy by showing a higher degree of disorder. On this basis, higher levels of solids should increase the extent of packing between particles and further stabilise the protein network thus accounting for the systematic increase in t_m from 27 to 62°C with polymer concentration, using as a marker the frequency dependent crossing of G'' and G'. By contrast, t_m values for maltodextrin networks range from about 70°C for the 15% preparation to >95°C for the 44% sample and beyond.

Figure 9 shows the concentration dependence of experimental and calculated elastic moduli for Promilk networks at 5°C, fitted with equation 1 (sum of squared differences is 0.1). Compared with the enthalpic, intermolecular associations of gelling polysaccharides and

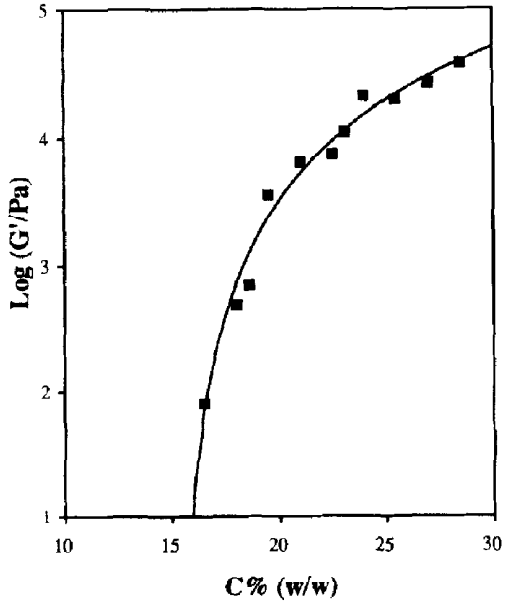

Fig. 9. The cascade fit of storage modulus for milk protein gels of Fig. 7 at the end of the isothermal run (5°C; 90 min).

gelatin, the attractive forces between neighbouring molecules of the denatured milk protein are rather weak as pointed out by the high value of minimum critical gelling concentration ($C_O \approx 15.3\%$) and the low functionality ($f = 2.7$). Differences in the gelling and melting profiles of C^*1906 and Promilk samples will be used to pin-point the phase-inversion composition from a protein to a maltodextrin continuous composite gel. Furthermore, the cascade fits of Figs 5 and 9 have been incorporated in a computerised algorithm in an attempt to elucidate the state of phase separation and the partition of solvent between the two polymeric components in the blend.

Mechanical properties of composite maltodextrin–milk protein gels

Binary systems were prepared from single stock solutions at 50°C. Upon mixing, solutions went cloudy, indicating that they consist of phase separated inclusions large enough to scatter visible light. Centrifugation of the samples (45°C, 15 min, 1150 **g**) resulted in bulk phase separation with a yellow bottom layer consisting predominantly of protein, and a translucent top layer being rich in maltodextrin.

Figure 10 shows the temperature course of gel formation in composite systems where the milk protein concentration was fixed at 16.5% and the amount of maltodextrin was allowed to vary from 0 to 18%. Clearly, two discrete types of modulus development emerge with increasing amounts of the polysaccharide in the blend. At the lower range of C^*1906 concentrations (up to 12%) the G' values increase monotonically as observed for the single protein networks (see also Fig. 7). Beyond this level however, the build up of structure in the mixtures follows the sigmoidal pattern recorded for the maltodextrin gels. Furthermore the sharp increase in modulus growth appears much earlier in the cooling cycle for the mixtures than for the individual maltodextrin preparations. Thus the onset of sigmoidal transition for a 13% C^*1906 gel has already started at about 15°C during the cooling ramp in Fig. 10, but it should emerge much later and well within the following isothermal run according to Fig. 2. This behaviour argues for dominant polymer exclusion phenomena which concentrate up the polysaccharide phase and in the case of the nominal concentration of 13% C^*1906 in Fig. 10, for example, gelation reproduces the enthalpic transition of the 24% one-component maltodextrin gel in Fig. 2.

Heating of the composite gels from 5 to 95°C at a scan rate of 1 deg/min produces the melting profiles of Fig. 11. A similar behaviour to that of the cooling scans is observed with the heating spectra falling into two distinct groups. Thus at maltodextrin concentrations between 0 and 12% in the blend, a smooth decrease in the values of storage modulus with temperature results in the early collapse of networks, e.g. at about 40, 60 and 70°C, typically illustrated for the 16.5% milk protein at 4, 8 and 12% maltodextrin, respectively. By contrast, the melting of protein networks at higher contents of maltodextrin (from 13 to 18%) weakens the gel, but then the values of shear moduli level off before their descent at higher temperatures associated with the melting of the individual maltodextrin networks. As illustrated for the samples of 16.5% protein and 13 or 18% C^*1906, there is residual structure even at the highest temperature accessible on the rheometer (95°C)

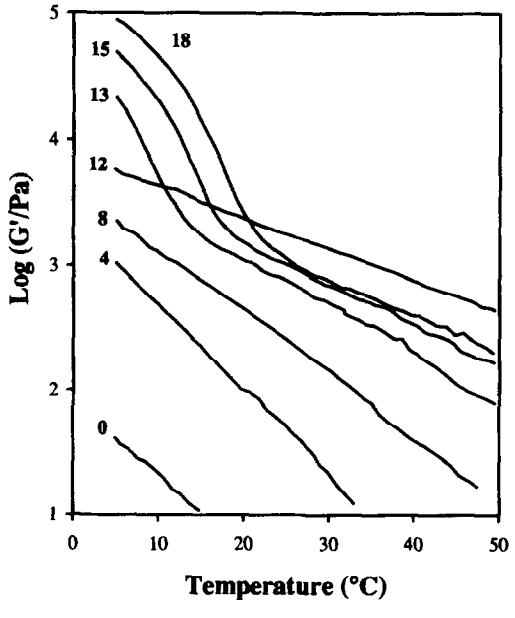

Fig. 10. Cooling profiles of G' for mixed systems of milk protein (16.5%) and maltodextrin (concentrations shown by the individual traces) at a scan rate of 1 deg/min.

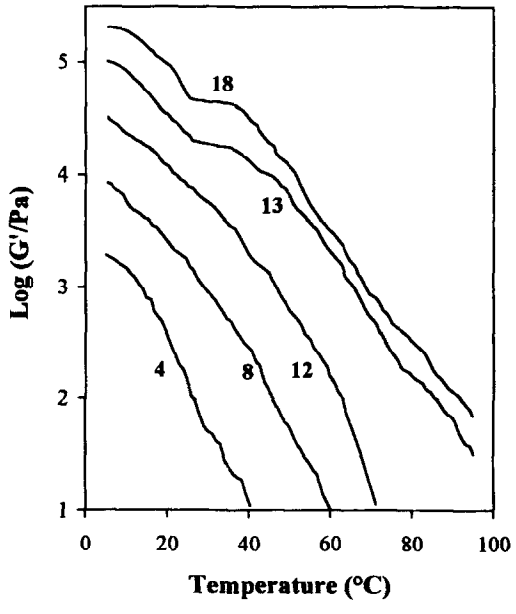

Fig. 11. Heating spectra of G' for mixed systems of milk protein (16.5%) and maltodextrin (concentrations shown by the individual traces) at a scan rate of 1 deg/min.

due to the thermally stable, amylose-like associations of the maltodextrin gels. In terms of the state of phase separation in the mixed system, the overriding conclusion to be drawn from the data of Figs 10 and 11 is that phase inversion from a continuous milk protein network with maltodextrin inclusions to an assembly in which maltodextrin forms the supporting phase with milk protein dispersed as the filler occurs at a nominal maltodextrin concentration between 12 and 13% in the composite gel.

Modelling of the phase behaviour in the maltodextrin–milk protein system

The blending laws of the Takayanagi model (1963) have been used to relate the concentration and the morphology of two component phases to the overall modulus of a composite biopolymer gel in the following mathematical expressions (Clark *et al.*, 1982, 1983):

$$G_c = \phi G_x + (1 - \phi)G_y \quad (2)$$

$$1/G_c = \phi/G_x + (1 - \phi)/G_y \quad (3)$$

where G_c, G_x and G_y are the moduli of the composite, X-phase and Y-phase polymers, respectively, and ϕ is the volume of phase X. For $G_x > G_y$ and the polymer X forming the supporting matrix, the above approach gives an isostrain or upper bound behaviour (eqn 2) whereas phase inversion in the system, with the polymer X being now the discontinuous filler, results in the so-called isostress or lower bound model (eqn 3).

Since at the moment there is no experimental technique for direct measurements of phase volumes in the gel state, a computerised algorithm was devised to consider all possible distributions of solvent between two polymeric components, with S_x and S_y being the solvent fractions in phases X and Y, respectively, so that S_x plus S_y is equal to one (Morris, 1992). For each combination of solvent fractions, the effective polymer concentration is calculated and then translated into values of G_x and G_y for substitution m the equations (2) and (3), by using similar relationships to the concentration-dependence of modulus defined in Figs 5 and 9. In the case of concentrated preparations, the direct contribution of polymer chains to phase volume was also taken into account for calculations of ϕ in the isostrain and isostress models (Kasapis *et al.*, 1993d). Figure 12 illustrates the variation in calculated moduli as a function of the fraction of solvent in the polymer X phase. As the value of S_x increases from 0 to 1, the calculated values of G_x decrease whereas those of G_y increase. A point is reached where the solvent partition between the polymers is such that the two curves cross, making the rigidity of the phases identical. At the same time the upper bound (X-continuous phase; isostrain conditions) descends from the top left corner of the diagram, with

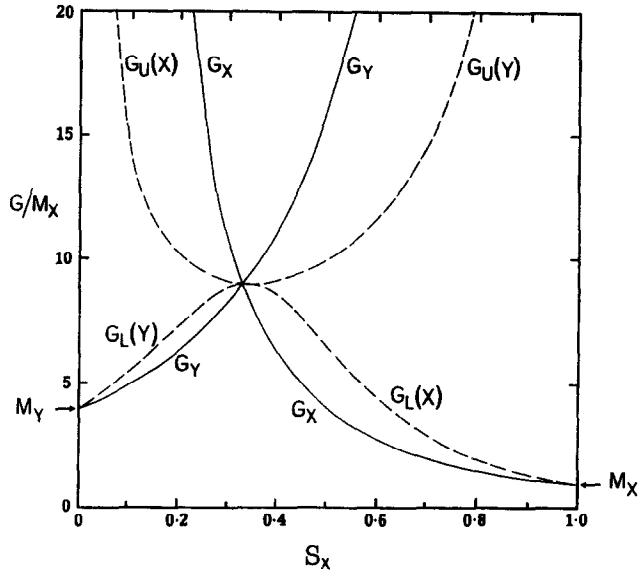

Fig. 12. Effect of solvent fraction in the polymer X-rich phase (S_x) on the value of calculated moduli (G/M_x). At their nominal concentrations, polymer X is four times stronger than X ($M_y = 4M_x$). Solid lines trace the variation in network strength of the individual components (G_x and G_y), whereas broken lines represent the shear moduli of the composite according to isostrain and isostress model (G_U and G_L, respectively). In both cases the continuous network is shown in brackets (with permission from Morris, 1992).

the lower bound (Y-continuous phase; isostress conditions) rising from the bottom left one, meeting again at the same critical point. Beyond this common point, the physical significance of the bounds swaps over, with the Y-continuous phase representing the upper bound (isostrain conditions) and with converse significance for the X-continuous phase (lower bound; isostress conditions).

Using the above framework, the quantitative analysis of the mechanical properties for the mixed gels of this investigation was carried out and its computerised output is presented in Fig. 13. In this illustration, calculated bounds for the 16.5% milk protein series are plotted against the solvent fraction in the protein phase (polymer X). From the evidence of gelling and melting profiles in Figs 10 and 11, experimental moduli for binary combinations up to 12% maltodextrin should be plotted on the milk protein continuous bounds which run from the top left to the bottom right corner of the graph. Since all experimental points intercept, the isostress part of the protein bounds the isostrain curves for this concentration range are not drawn to avoid clutter. For combinations beyond the phase inversion point, a maltodextrin continuous system is indicated and the moduli obtained for these composite gels should be plotted on the corresponding bounds which stretch from the bottom left to the top right corner of the same figure. In this case, only the upper bounds are shown, as the experimental points intercept the isostrain part of

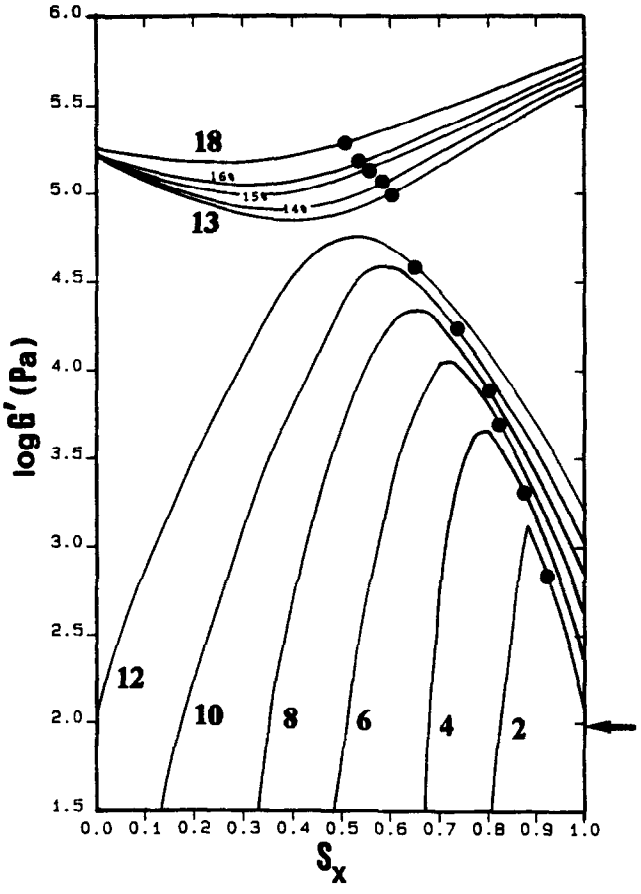

Fig. 13. Calculated bounds for the mixed gels of 16.5% w/w milk protein series as a function of solvent fraction in the protein phase (S_x). In the milk protein continuous systems (2–12% maltodextrin in the composite) only the lower bounds are drawn whereas at maltodextrin concentrations beyond the inversion point (13–18%) the isostrain predictions are illustrated. Experimental values are shown to intercept the bounds and the experimental modulus for 16.5% milk protein in isolation is noted by the arrow on the right-hand axis.

the maltodextrin continuous curve. Gratifyingly, increasing amounts of C^*1906 in the mixture claim, as we would expect, more and more of the solvent and result in smaller solvent fractions in the Promilk phase. Overall, experiment and theory argues that low maltodextrin concentrations in the blend (2–12%) allow the milk protein to form a weak network surrounding the stronger inclusions of the polysaccharide, whereas at higher levels of C^*1906 (13–18%), phase inversion occurs resulting in a strong maltodextrin matrix which is penetrated by the weaker protein filler.

Prediction of the variation in solvent fraction of the milk protein phase with maltodextrin concentration can be readily recast in the form of solvent partition between the two constituent polymers. A convenient parameter compares the amount of solvent kept in each phase per unit of the original (nominal) concentration of the appropriate polymer:

$$p = (S_x/x)/(S_y/y) \qquad (4)$$

where x and y are, respectively, the weights of polymers X and Y in the mixture. The parameter p was introduced by Clark *et al.* (1983) in the mechanical investigation of gelatin-agar blends at which the two biopolymers were assumed to gel separately within their own phases at thermodynamic equilibrium. The present investigation, however, incorporates the p concept in the bounds analysis in order to identify the driving force (kinetic influences or thermodynamic equilibrium) behind the state of phase separation in the maltodextrin–milk protein system. In Fig. 14, the composite bounds and storage moduli of Fig. 13 have been reproduced by plotting against p, derived from eqn (4). Clearly, there is a dramatic change in the distribution of solvent between the two phases as a result of phase inversion in the mixture with the values of p creating two families of points. Besides the step change in the partition of solvent between 12 and 13% C^*1906 in the sample, there is no systematic variation in p values within each group of data, with intercepts indicating that the protein holds 70% more solvent than the polysaccharide in the protein continuous gels ($\log p \approx 0.23$; $p \approx 1.7$), whereas this excess is reduced to only 10% when the milk protein forms the discontinuous filler ($\log p \approx 0.04$; $p \approx 1.1$).

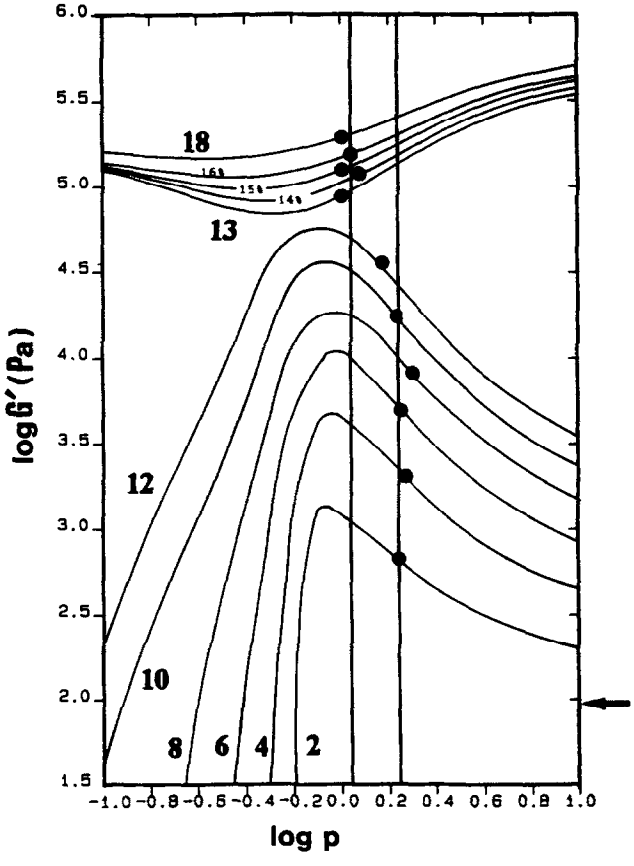

Fig. 14. Calculated lower or upper bounds for the 16.5% w/w milk protein with maltodextrin at concentrations (% w/w) shown, plotted as a function of the water partition parameter, p. Symbols as in Fig. 13.

The small deformation behaviour of maltodextrin–milk protein gels at isostress conditions was treated by the theoretical relationship of Kerner to predict the shape of filler particles in the blend (Nielsen, 1974). This equation relates the reinforcement ratio of elastic modulus in the composite (G_c) and matrix gel (G_m) to the phase volume of the rigid inclusions (ϕ_i), with the value of their maximum packing fraction (ϕ_m) giving an indication of the macromolecular arrangement of the discontinuous phase:

$$G_c/G_m = (1 + AB\phi_i)/(1 - B\psi\phi_i) \quad (5)$$

where

$$A = (7 - 5\mu)/(8 - 10\mu) \quad (6)$$

$$B = [(G_f/G_m) - 1]/[(G_f/G_m) + A] \quad (7)$$

and

$$\psi\phi_i = 1 - \exp\{-\phi_i/[1 - (\phi_i/\phi_m)]\} \quad (8)$$

In eqn (6) μ is the Poisson's ratio and the G_f in eqn (7) denotes the shear modulus of the filler particles. Extraction of solvent fractions from Fig. 13, or eqn (4) in combination with Fig. 14, allows the calculation of (Kasapis *et al.*, 1993d) effective concentrations, phase volumes and thus of real moduli for both matrix and filler in the nominal concentration range of maltodextrin from 0 to 12% (Table 1). The reinforcement ratios of experimental G_c to calculated G_m were compared with the theoretical reinforcement for a dispersed phase in the shape of spheres and rods. The maximum packing fraction of monodisperse spheres is taken as 0.64 whereas the ϕ_m values of highly polydisperse systems approximate 1. In the case of rods, traversing from a small to a large size distribution sees an increase in the ϕ_m values from 0.37 to 1. The factor A (eqn 6), depends heavily on the morphology of the mixture, and for a composite system with rigid spherical inclusions in a softer matrix it takes the value of 1.5. A filler phase in the shape of rods, yields values of A which increase with aggregate length, and they have been published for axial ratios from 4 to 15 (A is equal to 2.08 and 8.4, respectively).

Table 1 summarises the outcome of the application of the Kerner approach to the maltodextrin–milk protein co-gels at combinations before the phase inversion point. Parameters were used in eqn (5) for extraction of the theoretical reinforcement ratios and results are shown in Fig. 15. Experimental points fall closer to the calculated straight line for polydisperse spheres (ϕ_m = 1). The calculated curves correspond to polydisperse (ϕ_m = 1) and monodisperse (ϕ_m = 0.37) rods with an axial ratio of 15. Rods of shorter length produce fits which fall just below the curves shown for the corresponding size distribution. Therefore, it seems that the morphology of liquid maltodextrin droplets within the continuous protein solution, created by mechanical stirring at 50°C during sample preparation, persists in the gel-state with the maltodextrin forming roughly spherical inclusions which gives a rheology quite distinct from those of rod-shaped particles.

Table 1. A selection of experimental observations and parameters derived using the blending laws and the Kerner analyses for the 16.5% milk protein plus increasing amounts of maltodextrin (from 2 to 12%) mixtures. Milk protein is the continuous matrix (polymer X) whereas maltodextrin forms the discontinuous filler (polymer Y)

Maltodextrin:	2 (%)	4 (%)	6 (%)	8 (%)	10 (%)	12 (%)
S_x	0.92	0.87	0.82	0.79	0.73	0.65
C_x (%)	18.04	19.28	20.53	21.60	23.45	26.23
C_y (%)	23.47	27.75	30.55	33.86	33.77	32.35
ϕ_y	0.084	0.141	0.192	0.228	0.290	0.367
G_c (Pa)	731	1960	5711	7779	17 320	38 630
G_m (Pa)	719	1937	4372	6530	12 632	25 376
G_f (Pa)	34 120	102 553	166 886	260 905	257 734	215 694
A_s	1.5	1.5	1.5	1.5	1.5	1.5
B_s	0.949	0.954	0.937	0.940	0.886	0.750
$\Psi_{S0.64}$	0.092	0.165	0.240	0.298	0.412	0.580
Ψ_{S1}	0.088	0.151	0.212	0.256	0.335	0.439
A_{15R}	8.4	8.4	8.4	8.4	8.4	8.4
B_{15R}	0.832	0.847	0.798	0.806	0.674	0.443
$\Psi_{15R0.37}$	0.103	0.204	0.329	0.448	0.738	1.0
Ψ_{15R1}	0.088	0.151	0.212	0.256	0.335	0.440

$S_y = 1 - S_x$.
$\phi_x = 1 - \phi_y$.
A_s and B_s are the parameters from eqns (6) and (7) for spheres.
$\Psi_{S0.64}$ and Ψ_{S1} are the parameters of eqn (8) for spheres with ϕ_m of 0.64 and 1, respectively.
A_{15R} and B_{15R} are the parameters from eqns (6) and (7) for rods of axial ratio equal to 15.
$\Psi_{15R0.37}$ and Ψ_{15R1} are the parameters of eqn (8) of these rods with ϕ_m of 0.37 and 1, respectively.

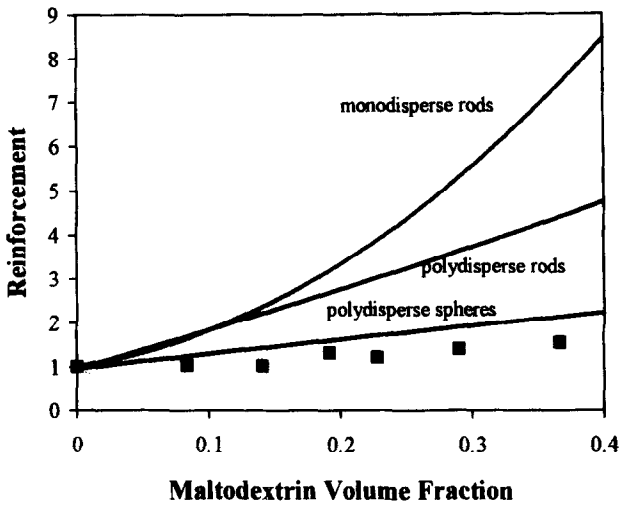

Fig. 15. Reinforcement of the composite gel with a milk protein continuous phase, i.e. at combinations below the phase inversion point. Extraction of phase volumes for maltodextrin concentrations between 0 and 12% in the mixed system allowed comparison of the experimental results (■) with the predicted behaviour obtained from the Kerner equation for spherical and rod-like inclusions of maltodextrin in the composite gel.

CONCLUSIONS

This work, in combination with the previous studies of gelatin–maltodextrin (Kasapis *et al.*, 1993d) and denatured milk–soya protein (Chronakis & Kasapis, 1993) systems, has contributed to a better understanding of the effect of polymer conformation on the state of phase separation in binary mixtures with relevance to the food industry. The emerging picture is as follows: conformationally similar species in solution like the disordered coils of gelatin and maltodextrin or the globular structures of milk and soya macromolecules tolerate each other at low concentrations in a monophasic solution. During cold-setting, the faster-gelling polymer in each mixture (gelatin or milk protein) develops its continuous network prior to ordering of the second component. Maltodextrin and soya protein upon ordering claim extra solvent and as a result deswell to a certain extent the gelatin and milk protein networks, but the systems remain under kinetic control as judged by repeated weighings of the mixtures which showed a continuous, slow diffusion of water from the faster to the slower setting component with time. In both systems, at higher concentrations (i.e. at combinations above the phase inversion point), the kinetic effect is swamped by the enthalpic disadvantage of polymer segments being surrounded by others of a different type and phase separation occurs in solution. This persists in the gel state and produces a single pattern of water partition throughout the concentration range (p is equal to 1.8 and 1.25 in favour of the gelatin and soya protein, respectively), but it is difficult to say if the systems have now reached thermodynamic equilibrium.

Dealing with the question of kinetic influences vs thermodynamic equilibrium in the present system, we have demonstrated that thermodynamic incompatibility between the conformationally dissimilar species of thermally-unfolded globular molecules of milk protein and disordered chains of maltodextrin promotes an early phase separation in solution and then in the gel state, i.e. at both sides of the phase inversion point. As a result there is an immediate reinforcing effect of the maltodextrin filler on the milk protein gel (Fig. 13) which was not observed in the case of gelatin and maltodextrin, where composite values below the phase inversion point remain close to that of the continuous gelatin network at its nominal concentration. Furthermore, the formation of milk protein or maltodextrin continuous gels allowed the resolution of two different patterns of water distribution in the blend. In particular, the proportion of solvent associated with the milk protein phase is reduced as it ceases to be the supporting phase and becomes the discontinuous filler. Having showed that the maltodextrin inclusions are roughly spherical we propose that the increase in the amount of solvent associated with the maltodextrin phase is due to phase inversion and the ensuing increase in its surface-to-volume ratio as the water tries to diffuse in the anisotropic medium. It follows that the difference in p values is the result of phase separated gels trapped away from equilibrium conditions, since the equilibrium value of "relative affinity" of the two polymers for water should not be affected by the geometrical rearrangements of their phases in a binary mixture. To make a last remark, both deswelled and phase separated networks seem to be under kinetic control with the solvent continuously seeking (but not achieving within the experimental time constraints) osmotic equilibrium and hence one might speculate that different rates of gelation (from quenching to controlled cooling) should reveal a trend in the partition of solvent between the constituent structures, in the development of composite modulus, and in the polymer composition at which phase inversion occurs.

ACKNOWLEDGEMENTS

The authors are grateful to Professor E.R. Morris/ Cranfield University for stimulating discussions, Professor J.R. Mitchell/University of Nottingham for critical evaluation of this manuscript and Dr F. Deleyn/ Cerestar for communication of unpublished results.

REFERENCES

Banach, G., Wesdorp, L.H. & Fiori, F.S. (1993). *United States Patent* **5**, 252, 352.

Chronakis, I.S. & Kasapis, S. (1993). *Food Hydrocoll.*, **7**, 459–478.

Clark, A.H. & Ross-Murphy, S.B. (1985). *Brit. Polym. J.*, **17**, 164–168.
Clark, A.H., Richardson, R.K, Ross-Murphy, S.B. & Stubbs, J.M. (1983). *Macromolecules*, **16**, 1367–1374.
Clark, A.H., Gidley, M.J, Richardson, R.K & Ross-Murphy, S.B. (1989). *Macromolecules*, **22**, 346–351.
Clark, A.H., Richardson, R.K., Robinson, G., Ross-Murphy, S.B. & Weaver, A.C. (1982). *Prog. Food Nutr. Sci.*, **6**, 149–160.
Daniels, S.C., Morrison, A. & Smith P.E. (1993). *International Patent* WO 93/17565.
Gidley, M.J. (1989). *Macromolecules*, **22**, 351–358.
Gidley, M.J. & Bulpin, P.V. (1987). *Carbohydr. Res.*, **161**, 291–300.
Hermansson, A.M. (1978). *J. Text. Studies*, **9**, 33–58.
Jane, J.-L. & Robyt, J.F. (1984). *Carbohydr. Res.*, **132**, 105–118.
Kasapis, S., Morris, E.R., Norton, I.T. & Clark, A.H. (1993a). *Carbohydr. Polym.*, **21**, 243–248.
Kasapis, S., Morris, E.R., Norton, I.T. & Gidley, M.J. (1993b). *Carbohydr. Polym.*, **21**, 249–259.
Kasapis, S., Morris, E.R., Norton, I.T. & Brown, C.R.T. (1993c). *Carbohydr. Polym.*, **21**, 261–268.
Kasapis, S., Morris, E.R., Norton, I.T. & Clark, A.H. (1993d). *Carbohydr. Polym.*, **21**, 269–276.
Manoj, P., Kasapis, S. & Chronakis, I.S. (1996). *Food Hydrocolloids*, in press.
Morris, E.R. (1992). *Carbohydr. Polym.*, **17**, 65–70.
Nielsen, L.E. (1974). *Rheol. Acta*, **13**, 86–92.
Ptitchkina, N.M., Danilova, I.A., Doxastakis, G., Kasapis, S. & Morris, E.R. (1994). *Carbohydr. Polym.*, **23**, 265–273.
Ross-Murphy, S.B. (1991). *Carbohydr. Polym.*, **14**, 281–294.
Takayanagi, M., Harima, H. & Iwata, Y. (1963). *Mem. Fac. Eng. Kyusha Univ.*, **23**, 1–13.